Occludin-deficient Embryonic Stem Cells Can Differentiate into Polarized Epithelial Cells Bearing Tight Junctions

Mitinori Saitou,* Kazushi Fujimoto,‡ Yoshinori Doi,*§ Masahiko Itoh,* Toyoshi Fujimoto,‖ Mikio Furuse,* Hiroshi Takano,¶ Tetsuo Noda,¶** and Shoichiro Tsukita***

*Department of Cell Biology, ‡Department of Anatomy, Faculty of Medicine, Kyoto University, Sakyo-ku, Kyoto 606, Japan; §Second Department of Internal Medicine, Osaka University Medical School, Suita, Osaka 565, Japan; ‖Department of Anatomy and Cell Biology, Gunma University School of Medicine, Showa-machi, Maebashi 371, Japan; ¶Department of Cell Biology, Cancer Institute, Toshima-ku, Tokyo 170, Japan; and **Department of Molecular Genetics, Tohoku University School of Medicine, Sendai 980, Japan

Abstract. Occludin is the only known integral membrane protein of tight junctions (TJs), and is now believed to be directly involved in the barrier and fence functions of TJs. Occludin-deficient embryonic stem (ES) cells were generated by targeted disruption of both alleles of the occludin gene. When these cells were subjected to suspension culture, they aggregated to form simple, and then cystic embryoid bodies (EBs) with the same time course as EB formation from wild-type ES cells. Immunofluorescence microscopy and ultrathin section electron microscopy revealed that polarized epithelial (visceral endoderm-like) cells were differentiated to delineate EBs not only from wild-type but also from occludin-deficient ES cells. Freeze fracture analyses indicated no significant differences in number or morphology of TJ strands between wild-type and occludin-deficient epithelial cells. Furthermore, zonula occludens (ZO)-1, a TJ-associated peripheral membrane protein, was still exclusively concentrated at TJ in occludin-deficient epithelial cells. In good agreement with these morphological observations, TJ in occludin-deficient epithelial cells functioned as a primary barrier to the diffusion of a low molecular mass tracer through the paracellular pathway. These findings indicate that there are as yet unidentified TJ integral membrane protein(s) which can form strand structures, recruit ZO-1, and function as a barrier without occludin.

THE establishment of compositionally distinct fluid compartments is of particular importance for the development and maintenance of multicellular organisms. Tight junctions (TJs),[1] which are located at the most apical region of epithelial and endothelial lateral membranes, play central roles in this compartmentalization by creating a primary barrier to the diffusion of solutes through the paracellular pathway (for reviews see Gumbiner, 1987, 1993; Schneeberger and Lynch, 1992). TJs are also thought to function as a boundary between the apical and basolateral plasma membrane domains, which differ in protein/lipid composition, to create and maintain epithelial and endothelial cell polarity (Rodriguez-Boulan and Nelson, 1989). These are known as the "barrier" and "fence" functions of TJs, respectively.

In ultrathin section electron micrographs, TJs appear as a series of discrete sites of apparent fusion, involving the outer leaflet of the plasma membranes of adjacent cells (Farquhar and Palade, 1963). By freeze fracture electron microscopy, these apparent fusion sites are observed as a set of continuous, anastomosing intramembranous particle strands (TJ strands) (Staehelin, 1973, 1974). Recent technical progress has enabled the identification of several TJ-associated peripheral membrane proteins such as zonula occludens (ZO)-1 (Stevenson et al., 1986), ZO-2 (Gumbiner et al., 1991), cingulin (Citi et al., 1988), 7H6 antigen (Zhong et al., 1993), and symplekin (Keon et al., 1996). Although detailed analyses of these proteins have led to better understanding of the structure and function of TJs, lack of information concerning the TJ-specific integral membrane proteins has hampered more direct assessment of the function of TJs at the molecular level. Recently, we identified occludin, an ~65-kD integral membrane protein, that is exclusively localized at the TJ strand in various epithelial and endothelial cells (Furuse et al., 1993).

Address all correspondence to Shoichiro Tsukita, Department of Cell Biology, Faculty of Medicine, Kyoto University, Sakyo-ku, Kyoto 606-01, Japan. Tel.: 81-75-753-4372. Fax: 81-75-753-4660. E-mail: htsukita@mfour.med.kyoto-u.ac.jp

1. *Abbreviations used in this paper*: AJ, adherens junction; E-cadherin, epithelial cadherin; EB, embryoid body; ES, embryonic stem; DKO, double knock-out; HBS, Hepes-buffered saline; pAb, polyclonal antibody; RT, reverse transcriptase; TJ, tight junctions; ZO, zonula occludens.

Occludin is thought to have four transmembrane domains in its NH_2-terminal half with both NH_2 and COOH termini located in the cytoplasm. Although the amino acid sequence of occludin is fairly diverse among distinct species, several structural aspects appear to be conserved phylogenetically; the high content of tyrosine and glycine residues in the first extracellular loop (~60%), low content of charged amino acid residues in the first as well as the second extracellular loops, and the possible coiled-coil formation of the long COOH-terminal cytoplasmic domain (Ando-Akatsuka et al., 1996).

Occludin is precisely colocalized with ZO-1 in various epithelial cells (Saitou et al., 1997), and its COOH-terminal region of ~150 amino acids specifically binds to ZO-1 in vitro (Furuse et al., 1994). In immuno-replica analyses, anti-occludin antibodies specifically labeled the TJ strand itself (Fujimoto, 1995; Furuse et al., 1996). When occludin was overexpressed in insect Sf9 cells, occludin was accumulated in the cytoplasmic vesicular structures to form characteristic multilamellar bodies, which bore apparent fusion sites as well as short TJ strand-like structures (Furuse et al., 1996). Furthermore, overexpression of occludin in cultured MDCK cells increased the number of TJ strands (McCarthy et al., 1996). These findings indicate that occludin plays a structural role in TJ formation; i.e., occludin is directly involved not only in the formation of TJ strands itself, but also in the linkage between TJ strands and the underlying cytoskeletons. Recently, TJ formation was shown to be regulated by the serine/threonine phosphorylation of occludin (Sakakibara et al., 1997).

Recent studies have suggested that occludin is also a functional component of TJs. Overexpression of full-length occludin in cultured MDCK cells elevated their transepithelial resistance (TER) (Balda et al., 1996; McCarthy et al., 1996), and introduction of COOH-terminally truncated occludin into MDCK cells or *Xenopus* embryo cells resulted in the increased paracellular leakage of small molecular mass tracers (Balda et al., 1996; Chen et al., 1997). The TER of cultured *Xenopus* epithelial cells was downregulated by addition to the culture medium of a synthetic peptide corresponding to the second extracellular loop of occludin (Wong and Gumbiner, 1997). In addition to these findings suggesting the involvement of occludin in the TJ barrier function, the TJ fence function was also shown to be affected when COOH-terminally truncated occludin was introduced into MDCK cells (Balda et al., 1996).

In this study, we knocked out both of the occludin alleles in embryonic stem (ES) cells by homologous recombination. The occludin-deficient ES cells aggregated to form cystic embryoid bodies in suspension culture, and their embryoid body formation ability was not different from that of wild-type ES cells. Occludin-deficient ES cells were differentiated into polarized epithelial cells delineating embryoid bodies, which bore well-developed TJs. ZO-1 was exclusively localized in TJ of occludin-deficient epithelial cells. Furthermore, TJs in occludin-deficient epithelial cells functioned as a primary barrier to the diffusion of a low molecular mass tracer through the paracellular pathway. These observations indicate the existence of other integral membrane protein component(s) of TJ strands, and we believe that this study provides new insight on our understanding of the structure and function of TJs.

Materials and Methods

Antibodies

Rat anti–mouse occludin mAb (MOC37) and rabbit anti–mouse occludin polyclonal antibody (pAb) (F4) were raised against the cytoplasmic domain of mouse occludin produced in *Escherichia coli* (Saitou et al., 1997; Sakakibara et al., 1997). Mouse anti–rat ZO-1 mAb (T8-754) was raised and characterized as described (Itoh et al., 1993). Rat anti–mouse E-cadherin mAb (ECCD2) was provided by Dr. M. Takeichi (Kyoto University, Kyoto, Japan).

Embryonic Stem Cell Culture and Embryoid Body Formation

J1 ES cells (Li et al., 1992) and their mutant clones were cultured on mouse embryonic feeder cells (Rudnicki et al., 1992) in high glucose DME (GIBCO BRL, Gaithersburg, MD) supplemented with 20% FCS, 0.1 mM 2-mercaptoethanol (Sigma Chemical Co., St. Louis, MO), 1,000 U/ml leukemia inhibitory factor (LIF) (Amrad Co., Kew, Victoria, Australia), 0.1 mM nonessential amino acids (ICN Biomedicals Inc., Costa Mesa, CA), 3 mM adenosine, 3 mM cytosine, 3 mM guanosine, 3 mM uridine, and 1 mM thymidine (Sigma Chemical Co.). For embryoid body formation, 6×10^6 ES cells were first cultured on gelatin-coated 10-cm culture dishes for 3 d in the same medium, and then subjected to suspension culture in three 10-cm bacterial dishes in the absence of LIF. The medium was changed every other day.

Targeting Vector

A λ phage 129/Sv mouse genomic library was screened using mouse occludin cDNA (nucleotides 1–424) as a probe, and then three overlapping clones were isolated. The overall structure of the mouse occludin genomic locus was determined by restriction and sequence analyses of these clones (see Fig. 1 *A*).

The targeting vector was designed to delete the entire sequence of exon 3 (273–945 nucleotides). A cassette consisting of SA (a splice acceptor sequence followed by triple splicing enhancers arranged in tandem [Friedrich and Soriano, 1991; Watakabe et al., 1993]), IRES (internal ribosomal entry sequence [Tsukiyama-Kohara et al., 1992]), LacZ (promoterless β-galactosidase sequence derived from pMC1871 [Pharmacia LKB Biotechnology, Uppsala, Sweden] that was preceded by a nuclear localization signal of SV-40 large T antigen [Kalderon et al., 1984]), loxP (Sternberg and Hamilton, 1981; Sauer and Henderson, 1988), *pgk* neo (Rudnicki et al., 1992), and loxP in this order was first constructed for positive selection. In this cassette, the *pgk* neo sequence was in the opposite orientation to the other sequences. A 7.5-kb BamHI fragment and a 1.8-kb HindIII–NheI fragment, which were located upstream and downstream from exon 3, were ligated upstream and downstream from the above cassette, respectively (see Fig. 1 *A*). A coding region of the diphtheria toxin A gene (Yagi et al., 1990) was then ligated downstream from the vector construct for negative selection against random integration of the vector.

Gene Targeting

The targeting vector was linearized at a unique NotI site located at the 5′ end of the 5′ homologous fragment, and then ES cells at passage 7–8 were electroporated with 20 μg of linearized targeting vector DNA using a Gene Pulser (Bio-Rad Laboratories, Hercules, CA) set at 400 V and 25 μF. Cells were plated on feeder cells in normal growth medium for 36–48 h, followed by selection with 175 μg/ml G418. Feeder cells were prepared from G418-resistant primary embryonic fibroblasts as described previously (Rudnicki et al., 1992). After 7–13 d, G418-resistant colonies were picked up and each colony was dissociated in Hepes-buffered saline (HBS) containing 0.1% trypsin and 1 mM EDTA, and then divided into two 96-well dishes. When each subclone became semiconfluent, cells in one well were frozen and those in the other well were used to isolate DNA for Southern blotting analysis (Laird et al., 1991). The colonies were screened individually by cleaving genomic DNA (15 μg) with XbaI and probing the Southern blots with 1-kb HindIII fragment just downstream from exon 4 (3′ probe). Correct targeting was confirmed by Southern blotting with an exon 2 probe (nucleotides 156–272) (5′ probe) (see Fig. 1 *A*). Targeted clones were also checked for single integration by hybridization with a neo probe.

To obtain occludin double knock-out ES cells, the single knock-out clones were plated at 6.0×10^6 cells/10-cm dish and cultured for 10 d with an elevated concentration of G418 (20 mg/ml). 48 clones survived, and Southern blotting analysis with a 3′ probe indicated that these included two independent occludin double knock-out cell lines (clones 23 and 29).

Reverse Transcriptase-PCR

Total RNA was isolated from ES cells or embryoid bodies using guanidine-thiocyanate and acid phenol/chloroform (Chomczymski and Sacchi, 1987) and cDNA was synthesized from 1 μg of total RNA using SuperScript II RNase H^- Reverse Transcriptase (RT; GIBCO BRL). Primers (upstream, 5′-TTGGGACAGAGGCTATGG-3′; downstream, 5′-ACCCACTCTTCAACATTGGG-3′) were designed to amplify a portion of occludin cDNA (nucleotide 487–1109). As a control for the presence of amplifiable RNA, hypoxanthine phosphoribosyl transferase primers were designed as previously described (Keller et al., 1993). PCR was performed in a 20-μl reaction volume containing 1 μg cDNA, 20 pmol of each primer, 0.25 mM of each dNTP, 1 unit of Taq polymerase (Boehringer Mannheim GmbH, Mannheim, Germany), and the buffer supplied by the manufacturer, under the following cycling conditions. For the occludin gene, an initial denaturation step of 3 min at 95°C was followed by 30 cycles of 1 min at 95°C, 1 min at 52°C, and 2 min at 72°C. The last cycle was followed by a further 10-min incubation at 72°C. Amplified PCR products were electrophoresed in 2% agarose gels and stained with ethidium bromide.

SDS-PAGE and Immunoblotting

ES cells and embryoid bodies were homogenized in 2× SDS sample buffer (50 mM Tris-HCl, pH6.8, 2% SDS, 20% glycerol, 2% 2-mercaptoethanol, 0.01% bromophenol blue) on ice, sonicated, and boiled for 10 min. Total lysate (20 μg) was resolved by SDS-PAGE (10%) based on the method of Laemmli (1970). Proteins were then electrophoretically transferred from gels onto nitrocellulose membranes, followed by incubation with anti-occludin pAb (F4). For antibody detection, a blotting detection kit with biotinylated immunoglobulin and alkaline phosphatase-conjugated streptavidin (Amersham International Plc., Little Chalfont, UK) was used.

Immunofluorescence Microscopy

Embryoid bodies were frozen in liquid nitrogen, and sectioned on a cryostat at a thickness of 10 μm. Sections were mounted on glass slides, air-dried, fixed in 95% ethanol at 4°C for 30 min, and then in 100% acetone at room temperature for 1 min. After rinsing in PBS (150 mM NaCl, 10 mM phosphate buffer, pH 7.5) containing 1% BSA for 15 min, sections were incubated with a mixture of rat anti-occludin mAb (MOC37) and mouse anti–ZO-1 mAb (T8-754), or a mixture of rat anti–E-cadherin mAb (ECCD 2) and mouse anti–ZO-1 mAb (T8-754) for 1 h. They were then washed three times with PBS containing 1% BSA and 0.1% Triton X-100, and incubated with second antibodies for 30 min. As second antibodies, a mixture of FITC-conjugated goat anti–rat IgG (TAGO, Inc., Burlingame, CA) and rhodamine-conjugated goat anti–mouse IgG (Amersham International Plc.) was used. After washing in PBS, samples were embedded in 90% glycerol-PBS containing 0.1% *para*-phenylendiamine and 1% *n*-propylgalate, and examined using an MRC 1024 confocal fluorescence microscope (Bio-Rad Laboratories) equipped with a Zeiss Axiophot II photomicroscope (Carl Zeiss, Inc., Thornwood, NY).

Ultrathin Section Electron Microscopy

Embryoid bodies were fixed with 2% paraformaldehyde and 2.5% glutaraldehyde in 0.1 M sodium cacodylate buffer, pH7.3, for 2 h at room temperature, followed by postfixation with 1% OsO_4 in the same buffer for 2 h on ice. Samples were stained en bloc with 0.2% uranyl acetate for 2 h at room temperature, dehydrated through a graded ethanol series, then embedded in Epon 812. Ultrathin sections were cut with a diamond knife, double stained with uranyl acetate and lead citrate, then examined using a 1200EX electron microscope (JEOL, Tokyo, Japan) at an accelerating voltage of 100 kV.

Freeze Fracture Electron Microscopy

For conventional freeze fracture analysis, embryoid bodies were fixed in 2% paraformaldehyde and 2.5% glutaraldehyde in 0.1 M sodium cacodylate buffer, pH 7.3, for 2 h at room temperature, immersed in 30% glycerol, and then frozen in liquid nitrogen. Frozen samples were fractured at −110°C and platinum-shadowed unidirectionally at an angle of 45° in Balzer's Freeze Etching System (BAF 400T; Balzers Corp., Hudson, NH). The samples were then immersed in household bleach, and replicas floating off the samples were washed with distilled water. Replicas were picked up on Formvar-filmed grids, and examined with a 1200EX electron microscope (JEOL) at an accelerating voltage of 80 kV.

The immunoelectron microscopic technique for examining freeze fracture replicas was described in detail previously (Fujimoto, 1995). Small pieces of cystic embryoid bodies were quickly frozen by contact with a pure copper block cooled with liquid helium gas (Heuser et al., 1979). Frozen samples were then fractured and shadowed as described above. The samples were immersed in sample lysis buffer containing 2.5% SDS, 10 mM Tris-HCl, and 0.6 M sucrose, pH 8.2, for 12 h at room temperature, then replicas floating off the samples were washed with PBS. Under these conditions, integral membrane proteins were captured by replicas, and their cytoplasmic domain was accessible to antibodies. The replicas were incubated with anti-occludin mAb MOC37 for 60 min, and then with goat anti–rat IgG coupled to 10-nm gold (Amersham International Plc.). The samples were washed with PBS and observed as described above.

Ultrathin Cryosection Immunoelectron Microscopy

Immunoelectron microscopy using ultrathin cryosections was performed essentially according to the method developed by Tokuyasu (1980; Fujimoto et al., 1992). Small pieces of embryoid bodies were fixed in 1% paraformaldehyde in 0.1 M phosphate buffer, pH 7.4, for 1 h at room temperature. Samples were then infused with 2 M sucrose containing 20% polyvinylpyrrolidone at 4°C overnight, rapidly frozen in liquid nitrogen, and then cut into ultrathin sections at −110°C using a diamond knife with an FC-4E low temperature sectioning system (Reichert-Jung, Vienna, Austria). Cryosections were collected on carbon-coated Formvar-filmed grids, washed six times with PBS containing 10 mM glycine (PBS-G), and incubated with PBS-G containing 1% BSA for 10 min. Sections were again washed with PBS-G four times and then incubated with mouse anti–ZO-1 mAb (T8-754) for 1 h. After washing with PBS containing 0.1% BSA seven times, sections were incubated with goat anti–mouse IgG coupled to 10-nm gold (Amersham International Plc.) for 1 h. They were washed with PBS containing 0.1% BSA seven times, and with PBS six times. They were then fixed with 2% glutaraldehyde in 0.1 M phosphate buffer, pH7.4, for 10 min, and then washed with distilled water six times, followed by staining with 2% methylcellulose containing 0.5% uranyl acetate for 10 min. Samples were air-dried and examined in a 1200EX electron microscope (JEOL) at an accelerating voltage of 80 kV.

Tight Junction Permeability Assay

Tight junction permeability assay using surface biotinylation technique was performed as described by Chen et al. (1997) with some modifications. Fully expanded wild-type and occludin-deficient cystic embryoid bodies were incubated in freshly made 1 mg/ml NHS-LC-biotin (Pierce Chemical Co., Rockford, IL) in HBS(+) (HBS containing 1 mM $CaCl_2$ and 1 mM $MgCl_2$) for 30 min. In some experiments, wild-type cystic embryoid bodies were incubated with 1 mg/ml NHS-LC-biotin in HBS containing 10 mM EGTA for 30 min at room temperature. After washing with HBS(+) three times, the surface-labeled embryoid bodies were fixed with 1% paraformaldehyde in 0.1 M phosphate buffer, pH 7.4, for 1 h at room temperature. Fixed samples were frozen in liquid nitrogen, and sectioned on a cryostat at a thickness of 12 μm. After rinsing in PBS containing 1% BSA for 1 h, sections were incubated for 1 h with a mixture of fluorescein-phalloidin (Pierce Chemical Co.) and XRITC-avidin (Pierce Chemical Co.), both of which were diluted 1:200 in PBS containing 1% BSA. The samples were embedded and examined by confocal fluorescence microscopy as described above.

Results

Targeted Disruption of Occludin Alleles in Embryonic Stem Cells

Occludin genomic clones were obtained by screening a λ phage 129/Sv mouse genomic library using mouse occludin cDNA fragment as a probe. From overlapping clones, the

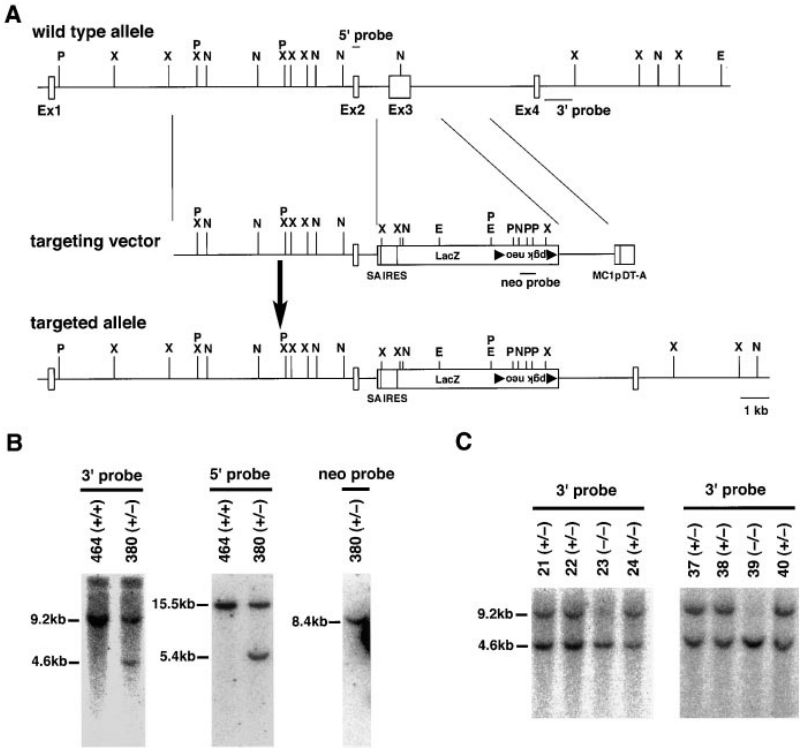

Figure 1. Targeted inactivation of the occludin gene in ES cells. (*A*) Restriction maps of the wild-type allele, the targeting vector, and the targeted allele of the occludin gene. The first ATG codon was located in exon 2; exon 3 encoded the NH_2-terminal half of occludin molecule from the first transmembrane domain to the second extracellular loop. Exon 4 encoded the fourth transmembrane domain and the initial part of the COOH-terminal cytoplasmic domain, indicating the existence of one or more downstream exons. The targeting vector contained the SA IRES/LacZ/loxP/*pgk* neo/loxP cassette in its middle portion to delete exon 3 in the targeted allele. The positions of 5′, 3′, and neo probes for Southern blotting are indicated as bars. The loxP sequence flanking *pgk* neo is shown by closed triangles. *P,* PstI; *X*, XbaI; *N*, NcoI; *E*, EcoRV. (*B*) Generation of occludin single knock-out ES cell lines. Southern blotting analysis of XbaI-digested occludin locus with 3′ probe (*3′ probe*) yielded a 9.2-kb band from the wild-type allele (clone *464*) and a 4.6-kb band from the targeted allele (clone *380*). The correct integration of the vector was confirmed by Southern blotting of PstI/EcoRV digest with 5′ probe (*5′ probe*). The 15.5- and 5.4-kb bands were derived from wild-type and targeted alleles, respectively. Furthermore, targeted clones were checked for single integration by hybridization with a neo probe (*neo probe*). (*C*) Generation of occludin double knock-out ES cell lines. Two independent double knock-out clones (clones *23* and *39*) were obtained from the single knock-out clone 380 in the presence of an elevated concentration of G418. The double knock-out cells lost the normal 9.2-kb band, indicating complete knock-out. Theoretically, it is possible that deleted COOH-terminal fragments of occludin (encoded by exons 4, 5 ---) are expressed in these cells, but these fragments, if any, are not regarded as structural or functional components of TJ strands.

genomic structure of the mouse occludin gene was partially clarified as shown in Fig. 1 *A*. The occludin gene contained at least five exons. The putative exon 2 contained the first ATG, exon 3 encoded the NH_2-terminal half of the occludin molecule from the first transmembrane domain to the second extracellular loop, and exon 4 encoded the fourth transmembrane domain and the initial part of the cytoplasmic tail. Considering that exon 5 was not found in the ~30-kb genomic DNA fragment that we obtained, the occludin gene was expected to be >30 kb.

In the targeting vector, a cassette of SA IRES/LacZ/loxP/*pgk* neo/loxP was flanked by upstream 7.5-kb and downstream 1.8-kb occludin DNA sequences (Fig. 1 *A*). The diphtheria toxin A gene driven by the MC1 promoter was ligated to the 3′ end of the construct to permit selection against random integration events. This targeting vector was designed with the expectation that homologous recombination between the vector and the occludin gene would result in deletion of exon 3, which consists of 673 bp (Fig. 1 *A*). The linearized targeting vector was introduced into ES cells, and cells were selected with G418. To screen for homologous recombination events, DNA from resistant clones were subjected to Southern blotting analysis with a probe corresponding to a sequence 3′ of the recombination site (3′ probe). The wild-type occludin allele displayed a 9.2-kb band on Southern blotting of XbaI-digested DNA, whereas the disrupted locus showed a 4.6-kb band (Fig. 1 *B*). Correct targeting was confirmed by Southern blotting with a 5′ probe, and targeted clones were also checked for single integration by hybridization with a neo probe. Of 200 G418-resistant clones examined, 9 had undergone a single homologous recombination event.

To prepare homozygous occludin-deficient cells (occludin double knock-out [DKO] cells), independent ES cell lines containing a single targeted occludin allele (6×10^6 cells for each line) were cultured in the presence of 20 mg/ml G418. Southern blotting analysis showed that 2 of 48 ES clones resistant to high concentrations of G418 had undergone gene conversion, resulting in disruption of both alleles (Fig. 1 *C*). These two independent occludin DKO clones (clone 23 and clone 39) showed the same growth rate with undifferentiated morphology in the absence of G418 (see Fig. 2 *A*, *e*). Since these two DKO clones showed the same phenotype as far as was examined, the data obtained from clone 23 are mostly represented below.

Formation of Embryoid Bodies from Occludin-deficient Embryonic Stem Cells

As previously reported (Doetschman et al., 1985; Baribault and Oshima, 1991), when wild-type ES cells were subjected to suspension culture, cells aggregated to form "embryoid body" structures (EBs) (Fig. 2 *A*, *a–d*). Within 2–4 d in suspension culture, the loose cellular aggregates became compact to form "simple EBs," delineated by an

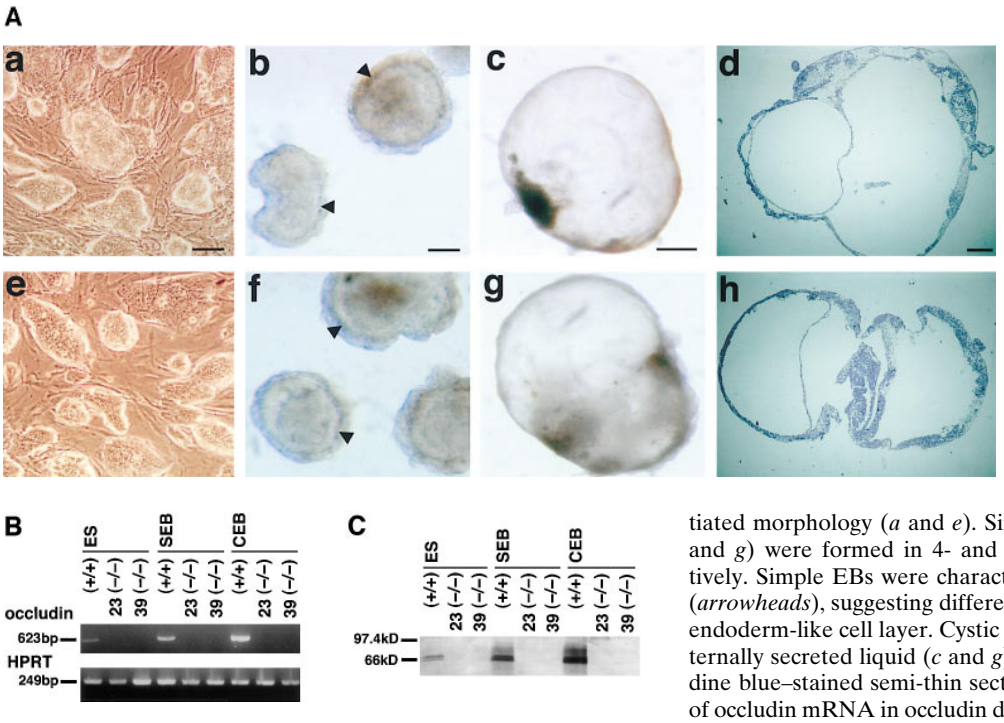

Figure 2. Embryoid body formation and occludin expression. (*A*) The appearance of ES cells (*a* and *e*), simple embryoid bodies (EBs) (*b* and *f*), and cystic EBs (*c*, *d*, *g*, and *h*) bearing homozygous wild-type (*a–d*) or targeted (*e–h*) occludin genes. No differences were detected between wild-type and occludin double knock-out ES cells/EBs, not only in their morphological appearance but also in the time course of EB formation. Regardless of occludin genotype, ES cells were grown on feeder cells with undifferentiated morphology (*a* and *e*). Simple (*b* and *f*) and cystic EBs (*c* and *g*) were formed in 4- and 10-d suspension culture, respectively. Simple EBs were characterized by Reichert's membranes (*arrowheads*), suggesting differentiation of the outermost visceral endoderm-like cell layer. Cystic EBs were fully expanded with internally secreted liquid (*c* and *g*), which was also shown on toluidine blue–stained semi-thin sectional images (*d* and *h*). (*B*) Loss of occludin mRNA in occludin double knock-out ES cells/EBs examined by RT-PCR. A trace amount of occludin mRNA was detected in wild-type ES cells (*ES*), and the amount appeared to increase as ES cells differentiated into simple EBs (*SEB*) and then into cystic EBs (*CEB*). In contrast, occludin expression was completely abolished in occludin double knock-out ES cells (clones *23* and *39*), simple, and cystic EBs. As a control, the hypoxanthine phosphoribosyl transferase gene was equally amplified in all samples. (*C*) Immunoblotting analyses with anti-occludin pAb. Consistent with the RT-PCR data, the protein expression level of occludin was elevated during the course of wild-type EB development, whereas no occludin expression was detected in occludin double knock-out ES cells/EBs. Bars: (*a*, *b*, *e*, and *f*) 100 μm; (*c* and *g*) 500 μm; (*d* and *h*) 200 μm.

outermost layer of epithelial cells (visceral endoderm-like cells) (Fig. 2 *A*, *b*). In suspension culture for a further 5 d, these simple EBs gradually expanded to form "cystic EBs" (Fig. 2 *A*, *c*). The cystic EBs contained large cavities filled with secreted fluid (Fig. 2 *A*, *d*). We examined whether occludin DKO ES cells can form simple and cystic EBs. As shown in Fig. 2 *A*, *f*, occludin DKO ES cells formed typical simple EBs within 2–4 d. Considering that so-called Reichert's membrane was detected in their outermost layer, it was suggested that an epithelial layer was induced on their surface. Surprisingly, with the same time course as wild-type simple EBs, these simple EBs of occludin DKO ES cells started to expand to form typical cystic EBs, which contained large cavities filled with secreted fluid (Fig. 2 *A*, *g* and *h*). These findings suggested the sealing activity of outermost epithelial cell layers of occludin DKO EBs.

Next, we confirmed the loss of occludin expression in occludin DKO cells through the course of EB formation (ES cells, 4-d simple EBs, and 10-d cystic EBs) at both mRNA and protein levels (Fig. 2, *B* and *C*). Expression of occludin mRNA was examined by RT-PCR using total RNA to amplify an occludin cDNA fragment encoding the region from the first to the fourth transmembrane domain (Fig. 2 *B*). An occludin cDNA fragment of the expected size was amplified from wild-type ES cells and their simple/cystic EBs, whereas no bands were detected from occludin DKO ES cells and their EBs (Fig. 2 *B*). We then performed immunoblotting analyses of these ES cells and EBs using anti-occludin pAb. Consistent with the RT-PCR data, a trace amount of occludin was detected in wild-type ES cells, and its protein expression level increased gradually during the formation and development of EBs (Fig. 2 *C*). Of course, occludin was not detected at the protein level in occludin DKO ES cells or their EBs.

The loss of occludin expression in occludin DKO EBs was also confirmed by immunofluorescence microscopy (Fig. 3). Double immunofluorescence microscopy of frozen sections of simple EBs derived from wild-type ES cells revealed precise colocalization of occludin and ZO-1 at junctional regions of the outermost epithelial cell layer (Fig. 3, *a–c*). In contrast, no occludin signal was detected from occludin DKO EBs, whereas intense ZO-1 signals were still detected from junctional regions of the outermost epithelial cell layer (Fig. 3, *d–f*). The expression level and subcellular distribution of E-cadherin did not appear to be affected in occludin DKO EBs (see Fig. 6). In wild-type cystic EBs, occludin and ZO-1 continued to be precisely colocalized at junctional regions of outermost epithelial cell layers, although some structures (probably premature blood vessels) were ZO-1–positive but occludin-negative (Fig. 3, *g–i*). In occludin DKO cystic EBs, occludin disappeared from junctional regions of the outermost epithelial cell layers without affecting the expression and distribution of ZO-1 (Fig. 3, *j–l*). These findings suggest that occludin-deficient cells can differentiate into polarized epithelial cells, and that even in occludin-deficient epithelial cells the structural integrity of intercellular junctions is maintained. We then evaluated this speculation at the electron microscopic level.

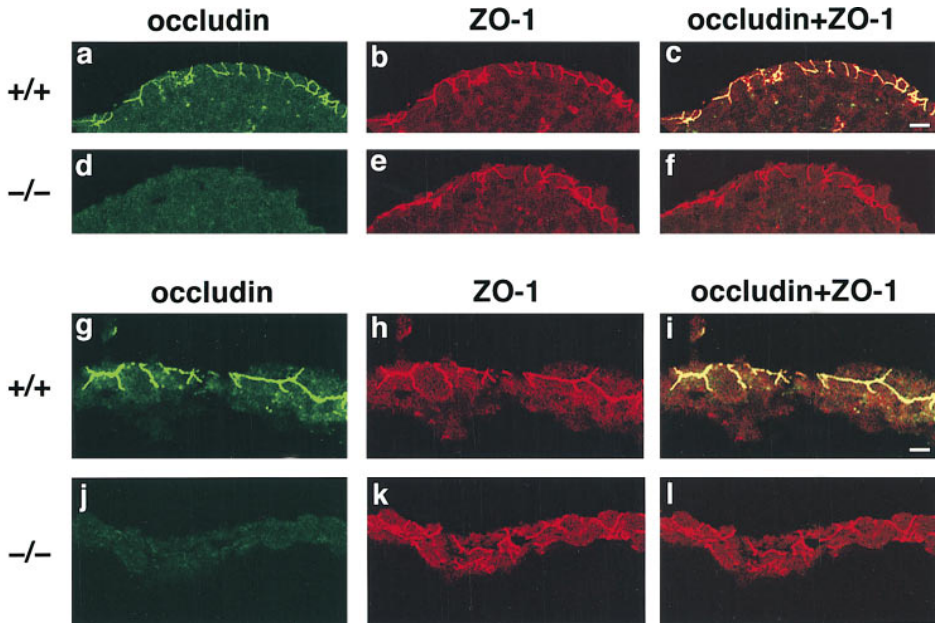

Figure 3. Immunofluorescence confocal microscopic localization of occludin and ZO-1 in wild-type and occludin-deficient simple EBs (*a–f*)/cystic EBs (*g–l*). Frozen sections of EBs were doubly stained with rat anti-occludin mAb (*a*, *d*, *g*, and *j*) and mouse anti–ZO-1 mAb (*b*, *e*, *h*, and *k*). In both wild-type simple (*a–c*) and cystic (*g–i*) EBs, occludin was specifically expressed in the outermost cell layers, and precisely colocalized with ZO-1 probably at junctional regions. In contrast, in occludin-deficient simple (*d–f*) and cystic (*j–l*) EBs, occludin disappeared from the outermost cell layers (*d* and *j*), and the loss of occludin expression did not appear to affect the distribution of ZO-1 (*e* and *k*). Bar, 10 μm.

Differentiation of Polarized Epithelial Cells from Occludin-deficient Embryonic Stem Cells

We first compared the morphology of the outermost cell layers delineating occludin-deficient simple/cystic EBs with that of wild-type EBs by ultrathin section electron microscopy (Fig. 4). As far as was examined, there were no differences between wild-type and occludin-deficient EBs. Both wild-type and occludin-deficient simple EBs were delineated by polarized epithelial cells, where apical membranes with microvilli and basal membranes with basement membranes were easily identified (Fig. 4, *a* and *b*). Regardless of the occludin expression, these epithelial cells were further differentiated into highly polarized epithelial cells (Fig. 4, *c* and *d*). These cells were characterized by numerous apical microvilli as well as many secretory granules that were arranged in a polarized manner. Typical TJ structures with discrete sites of apparent membrane fusion were well developed at the most apical region of lateral membranes of wild-type as well as occludin-deficient epithelial cells (Fig. 4, *e* and *f*).

We then examined the TJ structures in cystic EBs by conventional freeze fracture electron microscopy (Fig. 5). As expected, continuous and anastomosing TJ strands were detected in freeze fracture replica images of outermost epithelial cell layers of wild-type EBs, although the number of TJ strands significantly varied from cell to cell and from EB to EB (Fig. 5, *a* and *c*). Again, no morphological differences were detected in freeze fracture replica images of TJ between wild-type and occludin-deficient cystic EBs. The number of TJ strands in occludin-deficient epithelial cells appeared to be distributed within a similar range to that in wild-type cells (Fig. 5, *b* and *d*), and the morphological appearance of P-face TJ strands and complementary E-face TJ grooves was also indistinguishable between wild-type and occludin-deficient epithelial cells (Fig. 5, *e–h*). Of course, by immuno-freeze replica analysis, the TJ strands of wild-type cells were heavily labeled with anti-occludin mAb, whereas those of occludin-deficient cells were not labeled (Fig. 5, *i* and *j*). These findings indicated that occludin-deficient ES cells can differentiate into polarized epithelial cells, where TJs are normally formed without occludin.

Localization of ZO-1 in Epithelial Cells Differentiated from Occludin-deficient ES Cells

ZO-1 is known to be exclusively localized at TJs in epithelial cells expressing occludin, but to be localized in cadherin-based adherens junctions (AJs) in non-epithelial cells (Itoh et al., 1993, 1997). The existence of well-developed intercellular junctions in occludin-deficient epithelial cells led us to question whether the intense ZO-1 signal in these cells (see Fig. 3, *e* and *k*) was derived from TJ or AJ. Frozen sections of wild-type and occludin-deficient cystic EBs next were stained doubly with anti–E-cadherin and anti–ZO-1 mAbs, and observed by confocal microscopy. As shown in Fig. 6 *A*, the ZO-1 signal was detected more apically than the E-cadherin signal not only in wild-type but also in occludin-deficient epithelial cells. Considering that occludin and ZO-1 were precisely colocalized in wild-type epithelial cells, we concluded that ZO-1 still remained at TJ in occludin-deficient epithelial cells. Immunolocalization analysis using ultrathin cryosections confirmed the TJ-specific localization of ZO-1 in the occludin-deficient epithelial cells (Fig. 6 *B*).

Barrier Function of Tight Junctions Lacking Occludin

Finally, we examined the barrier function of TJs in occludin-deficient epithelial cells delineating cystic EBs. The tracer experiment procedure developed by Chen et al. (1997) gave reliable and reproducible results. This procedure was originally developed for evaluation of the paracellular leakage of epithelial cells in *Xenopus* embryos. Wild-type and occludin-deficient cystic EBs were suspended in isotonic solution containing NHS-LC-biotin, which covalently cross-links to an accessible cell surface,

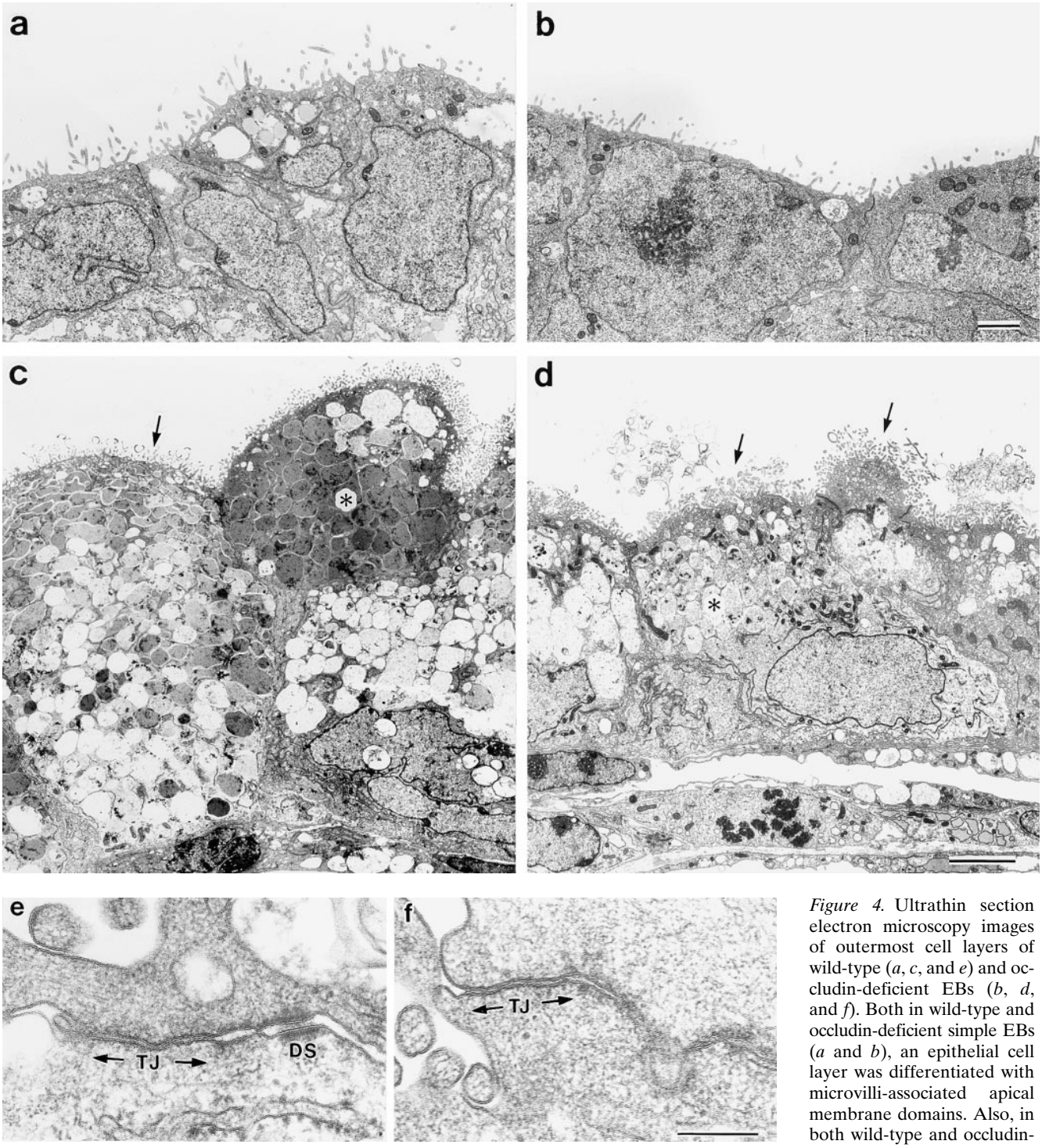

Figure 4. Ultrathin section electron microscopy images of outermost cell layers of wild-type (*a*, *c*, and *e*) and occludin-deficient EBs (*b*, *d*, and *f*). Both in wild-type and occludin-deficient simple EBs (*a* and *b*), an epithelial cell layer was differentiated with microvilli-associated apical membrane domains. Also, in both wild-type and occludin-deficient cystic EBs (*c–f*), the epithelial cells were further polarized with numerous microvilli (*arrows*) and secretory granules (*asterisks*). At the most apical region of the lateral membranes of these epithelial cells, well-developed tight junctions (*TJ*) were easily identified in wild-type (*e*) as well as occludin-deficient EBs (*f*). *DS*, desmosome. Bars: (*a* and *b*) 2 μm; (*c* and *d*) 7 μm; (*e* and *f*) 200 nm.

for 30 min, washed, and then fixed with formaldehyde. Frozen sections of these fixed samples were incubated with XRITC-avidin to detect bound biotin, and observed by confocal microscopy. As shown in Fig. 7, both in wild-type and occludin-deficient EBs, only the apical surfaces of the outermost epithelial cell layers, but never their basolateral surfaces, were labeled with biotin. When EBs were incubated with NHS-LC-biotin in the presence of 10 mM EGTA, intercellular junctions were partly affected, then basolateral membranes of outermost epithelial cell layers were occasionally biotinylated. Furthermore, when the incubation time was prolonged up to 1 h, the same results

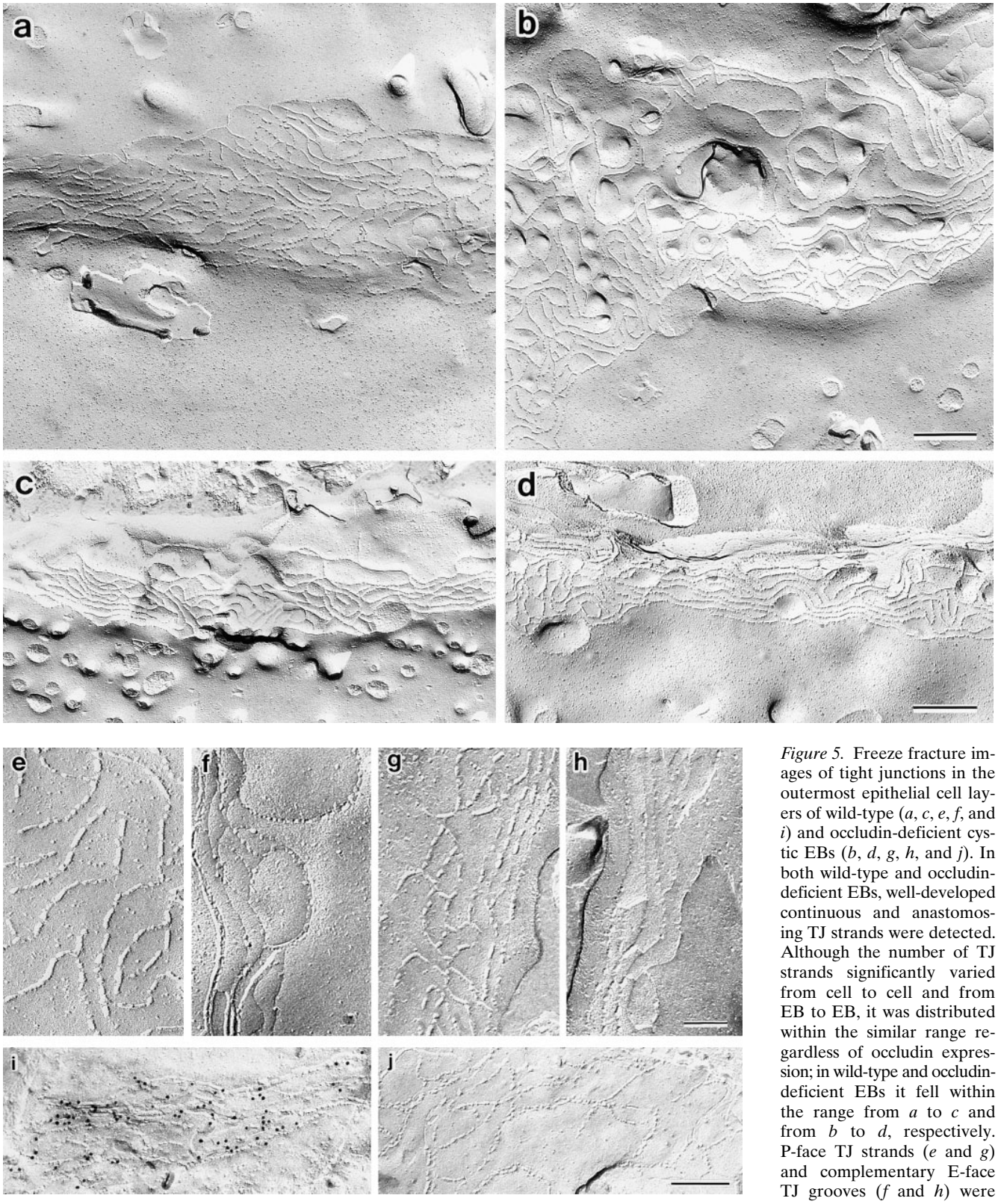

Figure 5. Freeze fracture images of tight junctions in the outermost epithelial cell layers of wild-type (*a*, *c*, *e*, *f*, and *i*) and occludin-deficient cystic EBs (*b*, *d*, *g*, *h*, and *j*). In both wild-type and occludin-deficient EBs, well-developed continuous and anastomosing TJ strands were detected. Although the number of TJ strands significantly varied from cell to cell and from EB to EB, it was distributed within the similar range regardless of occludin expression; in wild-type and occludin-deficient EBs it fell within the range from *a* to *c* and from *b* to *d*, respectively. P-face TJ strands (*e* and *g*) and complementary E-face TJ grooves (*f* and *h*) were also indistinguishable in their morphology between wild-type and occludin-deficient EBs. By immunoreplica electron microscopy, TJ strands of wild-type EBs (*i*) were heavily labeled with anti-occludin mAb, whereas those from occludin-deficient EBs (*j*) were not labeled. Bars: (*a–d*) 200 nm; (*e–h*) 50 nm; (*i–j*) 100 nm.

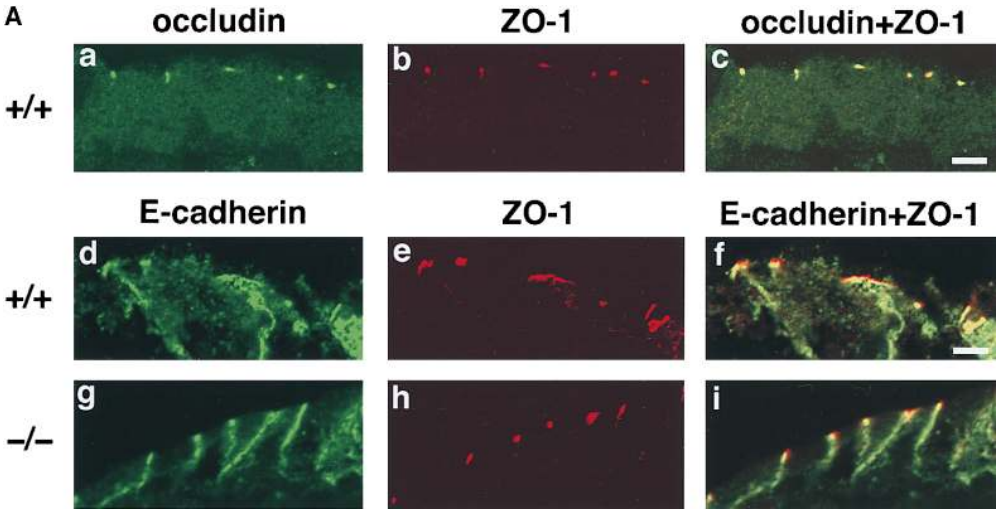

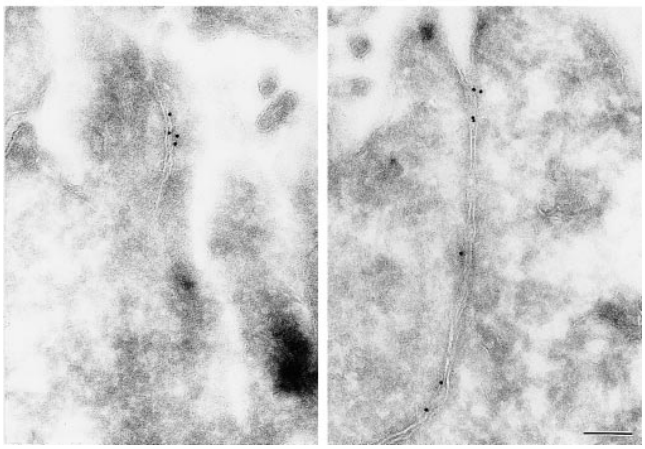

Figure 6. Subcellular distribution of ZO-1 in occludin-deficient epithelial cells. (*A*) Immunofluorescence confocal microscopy. Frozen sections of wild-type (*a–f*) and occludin-deficient (*g–i*) cystic EBs were doubly labeled with the mixture of rat anti-occludin mAb (*a*) and mouse anti–ZO-1 mAb (*b*) or the mixture of rat anti–E-cadherin mAb (*d* and *g*) and mouse anti–ZO-1 mAb (*e* and *h*). In wild-type EBs, E-cadherin was distributed along lateral membranes as well as at junctional regions (*d*), whereas occludin (*a*) and ZO-1 (*b* and *e*) were highly concentrated at junctional regions. Close comparison revealed that at junctional regions ZO-1 was precisely colocalized with occludin (*c*), but located more apically than E-cadherin (*f*). The same spatial relationship between E-cadherin (*g*) and ZO-1 (*h*) was maintained in occludin-deficient EBs (*i*). (*B*) Immunoelectron microscopy. Ultrathin cryosections of occludin-deficient cystic EBs were labeled with mouse anti–ZO-1 mAb. TJ was exclusively labeled. Bars: (*A*) 10 μm; (*B*) 200 nm.

were obtained (data not shown). These findings indicated that TJ lacking occludin can function as a primary barrier to paracellular leakage.

Discussion

Recent technical improvements have enabled disruption of both alleles of any gene in ES cells by homologous recombination (Thomas and Capecchi, 1987; Mortensen et al., 1992). When EBs were formed from ES cells by suspension culture, ES cells differentiated into polarized epithelial cells (visceral endoderm-like cells) on their surface (Doetschman et al., 1985; Baribault and Oshima, 1991). Thus, by inducing EBs from ES cells homozygous for any gene mutation, we can directly assess the role of the gene product in epithelial cell differentiation. In this study, we adopted this strategy to clarify the function of occludin, which is the only known integral membrane protein localized at TJs. Southern blotting and immunoblotting analyses showed that both alleles of the occludin gene were successfully knocked out in two independent ES cell lines. Surprisingly, both occludin-deficient ES cell lines differentiated into polarized epithelial cells, which bore well-developed TJ. We failed to detect any morphological differences in the epithelial cells or TJ structures between wild-type and occludin-deficient EBs. We thus concluded that there are as yet unidentified TJ integral membrane protein(s) that can form TJ strands, although it is not clear whether such proteins exist as primary components or as compensatory components to safeguard epithelial function in the event of genetic mutations. Of course, it is also possible that occludin-deficient TJ strands are composed of inverted cylindrical micelles of lipids as has long been assumed (Kachar and Reese, 1982; Pinto da Silva and Kachar, 1982; Verkleij, 1984), but even in this case, there should be some proteinous components that stabilize the lipid micelles (Stevenson and Goodenough, 1984; Stevenson et al., 1988).

This conclusion is consistent with recent observations suggesting the existence of TJ lacking occludin. For example, the introduction of COOH-terminally truncated occludin into MDCK cells redistributed endogenous occludin to be concentrated in a discontinuous dotted manner along the cell–cell border, whereas the continuous network of TJ strands was not affected (Balda et al., 1996). Furthermore, when a synthetic peptide corresponding to the second extracellular loop of occludin was added to the culture medium, it drove out the endogenous occludin from junctional areas of cultured epithelial cells without affecting the gross epithelial cell morphology (Wong and Gumbiner, 1997). Also under physiological conditions, en-

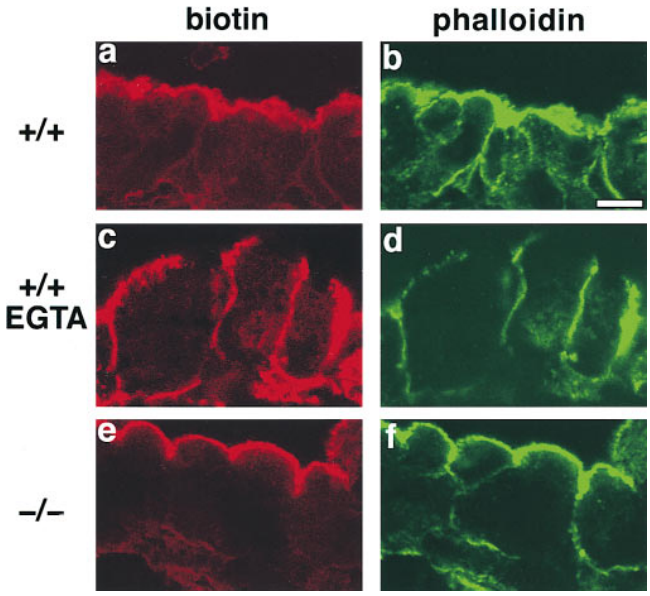

Figure 7. Tight junction permeability assay of wild-type and occludin-deficient epithelial cells. After wild-type (*a* and *b*) or occludin-deficient (*e* and *f*) cystic EBs were incubated with NHS-LC-biotin for 30 min, frozen sections were incubated with XRITC-avidin to localize surface-bound biotin (*a* and *e*). To visualize the contours of each epithelial cell, frozen sections were counterstained with fluorescein-phalloidin (*b*, *d*, and *f*). Regardless of occludin expression, only the apical surface of the outermost epithelial cell layer was biotinylated, indicating no paracellular leakage of NHS-LC-biotin. In contrast, when wild-type EBs were incubated with NHS-LC-biotin in the presence of 10 mM EGTA to affect intercellular junctions, the basolateral membranes as well as the apical membranes of epithelial cells were equally biotinylated (*c*). Bar, 10 μm.

dothelial cells in non-neuronal tissues bore TJ but expressed only trace amounts of occludin (Hirase et al., 1997).

On the other hand, the above conclusion cannot be easily reconciled with other recent observations. In immunoreplica analyses, TJ strands were heavily labeled with anti-occludin antibodies (Fujimoto et al., 1995; Saitou et al., 1997), and the expression level of occludin in various cells is correlated well with the number of TJ strands (Saitou et al., 1997). Furthermore, overexpression of occludin resulted in an increase in the number of TJ strands in MDCK cells (McCarthy et al., 1996) and in the formation of short TJ strand-like structures in Sf9 cells (Furuse et al., 1996). These findings indicate that occludin is at least one of the major constituents of TJ strands. However, the present study showed that TJ strands can be formed without occludin. Considering that cystic EBs delineated by well-polarized epithelial cells were normally formed from occludin-deficient ES cells, the barrier and fence functions of TJ did not appear to be affected by the homozygous elimination of the occludin gene. As compared with cultured simple epithelial cells such as MDCK cells, EBs were not appropriate for the detailed analysis of the TJ barrier and fence functions, partly because various types of cells were differentiated randomly in EBs, and partly because the size/developmental stage of each EB and the uniformity/continuity of outermost epithelial cell layers were uncontrollable. Within this limitation, we found in this study that the occludin-deficient TJ functioned as a primary barrier to the diffusion of a small molecular mass tracer, NHS-LC-biotin. In good agreement, recently occludin-deficient mice were normally born, suggesting that the homozygous elimination of the occludin gene does not affect the TJ functions that are required at least for embryogenesis (Saitou, M., H. Takano, M. Itoh, M. Furuse, Sh. Tsukita, and T. Noda, manuscript in preparation). In contrast, as described in the Introduction, recent studies with COOH-terminally truncated occludin or a synthetic peptide of the second extracellular loop have indicated that occludin is directly involved in the barrier function of TJ (Balda et al., 1996; Chen et al., 1997; Wong and Gumbiner, 1997).

Of course, the most simple explanation for these discrepancies is that there are several distinct but similar occludin isotypes, which are functionally redundant in terms of TJ strand formation, i.e., these occludin isotypes can be co-oligomerized into TJ strands. Indeed, in the case of connexin, a four-transmembrane protein constituting gap junctions, >10 isotypes have been identified, which are expressed in tissues in various combinations to form gap junctions by homo- and/or hetero-oligomerization (Jiang and Goodenough, 1996; Kumar and Gilula, 1996; Brink et al., 1997). Effects of homozygous gene knock-out of connexin isotypes on gap junction formation or function was, however, reported to be restricted in some specific tissues (Reaume et al., 1995; Nelles et al., 1996; Anzini et al., 1997; Simon et al., 1997). However, the existence of so-called isotypes of occludin is unexpected. Occludin isotypes have not been identified despite intensive efforts by PCR using various primers, and no sequences similar to occludin were found in the data bases. It is thus premature to further discuss the relationship between occludin and other putative integral membrane protein(s) in TJ strands.

Occludin has also been implicated in the recruitment of ZO-1 to TJs through the direct binding of its cytoplasmic domain to the NH_2-terminal half of ZO-1 (Furuse et al., 1994). In non-epithelial cells lacking occludin expression, ZO-1 was reported to be directly associated with α catenin and to be concentrated at cadherin-based AJs (Itoh et al., 1997). We thus expected that in occludin-deficient epithelial cells ZO-1 might be concentrated in AJs. Unexpectedly, however, ZO-1 was still localized exclusively in the occludin-deficient TJs. These findings indicate that in addition to occludin there are some other binding partner(s) for ZO-1 in TJs. Considering that ZO-1 is a multi-domain protein belonging to the MAGUK family (Woods and Bryant, 1993; Anderson et al., 1995; Kim, 1995), it is likely that ZO-1 binds to more than two distinct integral membrane proteins in TJ strands. For example, at neuronal post-synaptic densities, PSD-95, another MAGUK family member, was reported to cross-link the cytoplasmic domains of three distinct transmembrane proteins: the NMDA receptor, potassium channel, and neuroligin (Kim et al., 1995; Kornau et al., 1995; Niethammer et al., 1996; Irie et al., 1997).

The present study clearly revealed that the molecular architecture of TJ strands is more complex than expected; i.e., that occludin is not the only integral membrane protein of TJs. To understand the function of occludin and to understand the molecular architecture of TJ, we should first identify other novel integral membrane protein com-

ponent(s) of TJ strands. Identification of integral membrane proteins of TJ has been regarded as a difficult issue, but now we can use occludin as a probe to find such putative TJ components. Studies are currently underway along this line in our laboratory.

We thank all the members of our laboratory (Department of Cell Biology, Faculty of Medicine, Kyoto University) for helpful discussions.

This study was supported in part by a Grant-in-Aid for Cancer Research and a Grant-in-Aid for Scientific Research (A) from the Ministry of Education, Science and Culture of Japan.

Received for publication 16 December 1997 and in revised form 12 February 1998.

References

Anderson, J.M., A.S. Fanning, L. Lapierre, and C.M. Van Itallie. 1995. Zonula occludens (ZO)-1 and ZO-2: membrane-associated guanylate kinase homologues (MAGuKs) of the tight junction. *Biochem. Soc. Trans.* 23:470–475.

Ando-Akatsuka, Y., M. Saitou, T. Hirase, M. Kishi, A. Sakakibara, M. Itoh, S. Yonemura, M. Furuse, and Sh. Tsukita. 1996. Interspecies diversity of the occludin sequence: cDNA cloning of human, mouse, dog, and rat-kangaroo homologues. *J. Cell Biol.* 133:43–47.

Anzini, P., D.H.-H. Neuberg, M. Schachner, E. Nelles, K. Willecke, J. Zielasek, K.V. Toyka, U. Suter, and R. Martini. 1997. Structural abnormalities and deficient maintenance of peripheral nerve myelin in mice lacking the gap junction protein connexin 32. *J. Neurosci.* 17:4545–4551.

Balda, M.S., J.A. Whitney, C. Flores, S. González, M. Cereijido, and K. Matter. 1996. Functional dissociation of paracellular permeability and transepithelial electrical resistance and disruption of the apical-basolateral intramembrane diffusion barrier by expression of a mutant tight junction membrane protein. *J. Cell Biol.* 134:1031–1049.

Baribault, H., and R.G. Oshima. 1991. Polarized and functional epithelia can form after the targeted inactivation of both mouse keratin 8 alleles. *J. Cell Biol.* 115:1675–1684.

Brink, P.R., K. Cronin, K. Banach, E. Peterson, E.M. Westphale, K.H. Seul, S.V. Ramanan, and E.C. Beyer. 1997. Evidence for heteromeric gap junction channels formed from rat connexin43 and human connexin37. *Am. J. Physiol.* 273:1386–1396.

Chen, Y.-H., C. Merzdorf, D.L. Paul, and D.A. Goodenough. 1997. COOH terminus of occludin is required for tight junction barrier function in early *Xenopus* embryos. *J. Cell Biol.* 138:891–899.

Chomczymski, P., and N. Sacchi. 1987. Single-step method of RNA isolation by acid guanidium thiocyanate-phenol-chloroform extraction. *Anal. Biochem*. 162:156–159.

Citi, S., H. Sabanay, R. Jakes, B. Geiger, and J. Kendrick-Jones. 1988. Cingulin, a new peripheral component of tight junctions. *Nature.* 333:272–276.

Doetschman, T.C., H. Eistetter, M. Katz, W. Schmidt, and R. Kemler. 1985. The *in vitro* development of blastocyst-derived embryonic stem cell lines: formation of visceral yolk sac, blood islands and myocardium. *J. Embryol. Exp. Morph.* 87:27–45.

Farquhar, M.G., and G.E. Palade. 1963. Junctional complexes in various epithelia. *J. Cell Biol.* 17:375–412.

Friedrich, G., and P. Soriano. 1991. Promoter traps in embryonic stem cells: a genetic screen to identify and mutate developmental genes in mice. *Genes Dev*. 5:1513–1523.

Fujimoto, K. 1995. Freeze-fracture replica electron microscopy combined with SDS digestion for cytochemical labeling of integral membrane proteins. Application to the immunogold labeling of intercellular junctional complexes. *J. Cell Sci.* 108:3443–3449.

Fujimoto, T., S. Nakade, A. Miyawaki, K. Mikoshiba, and K. Ogawa. 1992. Localization of inositol 1,4,5-trisphosphate receptor-like protein in plasmalemmal caveolae. *J. Cell Biol.* 119:1507–1513.

Furuse, M., T. Hirase, M. Itoh, A. Nagafuchi, S. Yonemura, Sa. Tsukita, and Sh. Tsukita. 1993. Occludin: A novel integral membrane protein localizing at tight junctions. *J. Cell Biol.* 123:1777–1788.

Furuse, M., M. Itoh, T. Hirase, A. Nagafuchi, S. Yonemura, Sa. Tsukita, and Sh. Tsukita. 1994. Direct association of occludin with ZO-1 and its possible involvement in the localization of occludin at tight junctions. *J. Cell Biol.* 127: 1617–1626.

Furuse, M., K. Fujimoto, N. Sato, T. Hirase, Sa. Tsukita, and Sh. Tsukita. 1996. Overexpression of occludin, a tight junction-associated integral membrane protein, induces the formation of intracellular multilamellar bodies bearing tight junction-like structures. *J. Cell Sci.* 109:429–435.

Gumbiner, B. 1987. Structure, biochemistry, and assembly of epithelial tight junctions. *Am. J. Physiol.* 253:C749–C758.

Gumbiner, B.M. 1993. Breaking through the tight junction barrier. *J. Cell Biol.* 123:1631–1633.

Gumbiner, B., T. Lowenkopf, and D. Apatira. 1991. Identification of a 160kDa polypeptide that binds to the tight junction protein ZO-1. *Proc. Natl. Acad. Sci. USA*. 88:3460–3464.

Heuser, J.E., T.S. Reese, M.J. Dennis, Y. Jan, L. Yan, and L. Evans. 1979. Synaptic vesicle exocytosis captured by quick freezing and correlated with quantal transmitter release. *J. Cell Biol.* 81:275–300.

Hirase, T., J.M. Staddon, M. Saitou, Y. Ando-Akatsuka, M. Itoh, M. Furuse, K. Fujimoto, Sh. Tsukita, and L.L. Rubin. 1997. Occludin as a possible determinant of tight junction permeability in endothelial cells. *J. Cell Sci.* 110:1603–1613.

Irie, M., Y. Hata, M. Takeuchi, K. Ichtchenko, A. Toyoda, K. Hirao, Y. Takai, T.W. Rosahl, and T.C. Südhof. 1997. Binding of Neuroligins to PSD-95. *Science.* 277:1511–1515.

Itoh, M., A. Nagafuchi, S. Yonemura, T. Kitani-Yasuda, Sa. Tsukita, and Sh. Tsukita. 1993. The 220-kD protein colocalizing with cadherins in non-epithelial cells is identical to ZO-1, a tight junction-associated protein in epithelial cells: cDNA cloning and immunoelectron microscopy. *J. Cell Biol.* 121:491–502.

Itoh, M., A. Nagafuchi, S. Moroi, and Sh. Tsukita. 1997. Involvement of ZO-1 in cadherin-based cell adhesion through its direct binding to α catenin and actin filaments. *J. Cell Biol.* 138:181–192.

Jiang, J.X., and D.A. Goodenough. 1996. Heteromeric connexons in lens gap junction channels. *Proc. Natl. Acad. Sci. USA*. 93:1287–1291.

Kachar, B., and T.S. Reese. 1982. Evidence for the lipidic nature of tight junction strands. *Nature.* 296:464–466.

Kalderon, D., B.L. Roberts, W.D. Richardson, and A.E. Smith. 1984. A short amino acid sequence able to specify nuclear location. *Cell.* 39:499–509.

Keller, G., M. Kennedy, T. Papayannopoulou, and M.V. Wiles. 1993. Hematopoietic commitment during embryonic stem cell differentiation in culture. *Mol. Cell. Biol.* 13:473–486.

Keon, B.H., S. Schäfer, C. Kuhn, C. Grund, and W.W. Franke. 1996. Symplekin, a novel type of tight junction plaque protein. *J. Cell Biol.* 134:1003–1018.

Kim, S.K. 1995. Tight junctions, membrane-associated guanylate kinases and cell signaling. *Curr. Opin. Cell Biol.* 7:641–649.

Kim, E., M. Niethammer, A. Rothschild, Y.N. Jan, and M. Sheng. 1995. Clustering of shaker-type K^+ channels by interaction with a family of membrane-associated guanylate kinases. *Nature.* 378:85–88.

Kornau, H.-C., L.T. Schenker, M.B. Kennedy, and P.H. Seeburg. 1995. Domain interaction between NMDA receptor subunits and the postsynaptic density protein PSD-95. *Science.* 269:1737–1740.

Kumar, N.M., and N.B. Gilula. 1996. The gap junction communication channel. *Cell.* 84:381–388.

Laemmli, U.K. 1970. Cleavage of structural proteins during the assembly of the head of bacteriophage T4. *Nature.* 227:680–685.

Laird, P.W., A. Zijderveld, K. Linders, M.A. Rudnicki, R. Jaenisch, and A. Berns. 1991. Simplified mammalian DNA isolation procedure. *Nucleic Acids Res.* 19:4293.

Li, E., T.H. Bestor, and R. Jaenisch. 1992. Targeted mutation of the DNA methyltransferase gene results in embryonic lethality. *Cell.* 69:915–926.

McCarthy, K.M., I.B. Skare, M.C. Stankewich, M. Furuse, Sh. Tsukita, R.A. Rogers, R.D. Lynch, and E.E. Schneeberger. 1996. Occludin is a functional component of the tight junction. *J. Cell Sci.* 109:2287–2298.

Mortensen, R.M., D.A. Conner, S. Chao, A.A.T. Geisterfer-Lowrance, and J.G. Seidman. 1992. Production of homozygous mutant ES cells with a single targeting construct. *Mol. Cell. Biol.* 12:2391–2395.

Nelles, E., C. Butzler, D. Jung, A. Temme, H.D. Gabriel, U. Dahl, O. Traub, F. Stumpel, K. Jungermann, J. Zielasek, K.V. Toyka, R. Dermietzel, and K. Willecke. 1996. Defective propagation of signals generated by sympathetic nerve stimulation in the liver of connexin32-deficient mice. *Proc. Natl. Acad. Sci. USA*. 93:9565–9570.

Niethammer, M., E. Kim, and M. Sheng. 1996. Interaction between the C terminus of NMDA receptor subunits and multiple members of the PSD-95 family of membrane-associated guanylate kinases. *J. Neurosci.* 16:2157–2163.

Pinto da Silva, P., and B. Kachar. 1982. On tight-junction structure. *Cell.* 28: 441–450.

Reaume, A.G., P.A. de Sousa, S. Kulkarni, B.L. Langille, D. Zhu, T.C. Davies, S.C. Juneja, G.M. Kidder, and J. Rossant. 1995. Cardiac malformation in neonatal mice lacking connexin 43. *Science.* 267:1831–1834.

Rodriguez-Boulan, E., and W.J. Nelson. 1989. Morphogenesis of the polarized epithelial cell phenotype. *Science.* 245:718–725.

Rudnicki, M.A., T. Braun, S. Hinuma, and R. Jaenisch. 1992. Inactivation of *MyoD* in mice leads to up-regulation of the myogenic HLH gene *myf-5* and results in apparently normal muscle development. *Cell.* 71:383–390.

Saitou, M., Y. Ando-Akatsuka, M. Itoh, M. Furuse, J. Inazawa, K. Fujimoto, and Sh. Tsukita. 1997. Mammalian occludin in epithelial cells: its expression and subcellular distribution. *Eur. J. Cell Biol.* 73:222–231.

Sakakibara, A., M. Furuse, M. Saitou, Y. Ando-Akatsuka, and Sh. Tsukita. 1997. Possible involvement of phosphorylation of occludin in tight junction formation. *J. Cell Biol.* 137:1393–1401.

Sauer, B., and N. Henderson. 1988. Site-specific DNA recombination in mammalian cells by the Cre recombinase of bacteriophage P1. *Proc. Natl. Acad. Sci. USA*. 85:5166–5170.

Schneeberger, E.E., and R.D. Lynch. 1992. Structure, function, and regulation of cellular tight junctions. *Am. J. Physiol.* 262:L647–L661.

Simon, A.M., D.A. Goodenough, E. Li, and D.L. Paul. 1997. Female infertility in mice lacking connexin 37. *Nature.* 385:525–529.

Staehelin, L.A. 1973. Further observations on the fine structure of freeze-cleaved tight junctions. *J. Cell Sci.* 13:763–786.

Staehelin, L.A. 1974. Structure and function of intercellular junctions. *Int. Rev. Cytol.* 39:191–283.
Sternberg, N., and D. Hamilton. 1981. Bacteriophage P1 site-specific recombination. I. Recombination between loxP sites. *J. Mol. Biol.* 150:467–486.
Stevenson, B.R., and D.A. Goodenough. 1984. *Zonulae occludentes* in junctional complex-enriched fractions from mouse liver: Preliminary morphological and biochemical characterization. *J. Cell Biol.* 98:1209–1221.
Stevenson, B.R., J.D. Siliciano, M.S. Mooseker, and D.A. Goodenough. 1986. Identification of ZO-1: A high molecular weight polypeptide associated with the tight junction (zonula occludens) in a variety of epithelia. *J. Cell Biol.* 103:755–766.
Stevenson, B.R., J.M. Anderson, and S. Bullivant. 1988. The epithelial tight junction: structure, function and preliminary biochemical characterization. *Mol. Cell. Biochem.* 83:129–145.
Thomas, K.R., and M.R. Capecchi. 1987. Site-directed mutagenesis by gene targeting in mouse embryo-derived stem cells. *Cell.* 51:503–512.
Tokuyasu, K.T. 1980. Immunochemistry on ultrathin frozen sections. *Histochem. J.* 12:381–403.
Tsukiyama-Kohara, K., N. Iizuka, M. Kohara, and A. Nomoto. 1992. Internal ribosome entry site within hepatitis C virus RNA. *J. Virol.* 66:1476–1483.
Verkleiji, A.J. 1984. Lipidic intramembranous particles. *Biochem. Biophys. Acta A.* 779:43–63.
Watakabe, A., K. Tanaka, and Y. Shimura. 1993. The role of exon sequences in splice site section. *Genes Dev.* 7:407–418.
Wong, V., and B.M. Gumbiner. 1997. A synthetic peptide corresponding to the extracellular domain of occludin perturbs the tight junction permeability barrier. *J. Cell Biol.* 136:399–409.
Woods, D.A., and P.J. Bryant. 1993. ZO-1, DlgA and PSD95/SAP90: homologous proteins in tight, septate and synaptic cell junctions. *Mech. Dev.* 44:85–89.
Yagi, T., Y. Ikawa, K. Yoshida, Y. Shigetani, N. Takeda, I. Mabuchi, T. Yamamoto, and S. Aizawa. 1990. Homologous recombination at *c-fyn* locus of mouse embryonic stem cells with use of diphtheria toxin A-fragment gene in negative selection. *Proc. Natl. Acad. Sci. USA.* 87:9918–9922.
Zhong, Y., T. Saitoh, T. Minase, N. Sawada, K. Enomoto, and M. Mori. 1993. Monoclonal antibody 7H6 reacts with a novel tight junction-associated protein distinct from ZO-1, cingulin, and ZO-2. *J. Cell Biol.* 120:477–483.